Design, production and reverse engineering of a double sided innovative thin film laser element

Michael Trubetskov*[a,b], Tatiana Amotchkina[b], Alexander Tikhonravov[b], Laszlo Veisz[a], Vladimir Pervak[c]
[a]Max-Planck-Institut für Quantenoptik, Hans-Kopfermann str. 1, 85748 Garching, Germany;
[b]Research Computing Center, Moscow State University, Leninskie Gory, 119991, Moscow, Russia;
[c]Ludwig-Maximilians-Universität München, Am Coulombwall 1, 85748 Garching, Germany

ABSTRACT

In the present work, an innovative optical element developed for the multiterawatt few-cycle light wave synthesizer based on optical parametric amplification is demonstrated. The synthesizer currently produces sub-5-fs, 80-mJ, 18-TW pulses. The required element had to be deposited on 15 mm substrate having 75 mm in diameter; an average value of the GDD of +75 fs^2 and reflectance exceeding 99% in the spectral wavelength region from 570 to 1030 nm.

Mechanical stresses of the designed dispersive mirror (DM) caused the substrate bending that distorts wave front quality resulting in the distorting of the beam waveform of laser system. In order to compensate this mechanical stress, the substrate back side was covered by an antireflection coating providing the lowest possible reflection in the working spectral range, having the total physical thickness close to DM thickness and total thicknesses of Nb_2O_5/SiO_2 layers close to the corresponding total thicknesses of Nb_2O_5/SiO_2 in DM. The produced DM-AR optical element exhibits excellent spectral properties.

Keywords: ultrafast coating, dispersive mirror, reverse engineering, coating design, stress compensation, pulse compression.

1. INTRODUCTION

Most of the modern ultrafast laser systems include thin film optical elements such as dispersive mirrors, chirped mirrors, beamsplitters, output couplers exploited for accurate phase control which is necessary for efficient pulse compression[1–5]. Design and production of such coatings require using effective numerical design algorithms, stable deposition techniques and high precision thickness control. In more challenging situations if, for some reasons, a double-sided thin film element is required, design, deposition and characterization of two complicated coatings should be interconnected.

An innovative optical element presented in this work has been developed for the multiterawatt few-cycle light wave synthesizer (LWS-20) based on optical parametric amplification. LWS-20 currently produces sub-5-fs, 80-mJ, 18-TW pulses. The required multilayer element had to have an average value of the GDD of +75 fs^2 and reflectance exceeding 99% in the spectral wavelength region from 570 to 1030 nm. Also, the element had to have the diameter of 75 mm at a substrate with 15 mm thickness.

Due to mechanical stresses of DM layers the substrate becomes bended, that distorts wave front quality resulting in the distorting of the beam waveform of laser system. To compensate this stress the substrate back side has been coated with a coating having approximately the same mechanical stress. The similar approach was applied in Ref. [6]. As the result, the surface flatness of the substrate will not be degraded. The back side of the sample is to be covered by an antireflection (AR) coating providing the lowest possible reflection in the working spectral range of the DM. If the sample back side is coated with AR coating having total physical thicknesses of each layer material close to the total physical thicknesses of the same materials in DM, stress compensation goal will be automatically achieved.

Except the important condition that AR coating thickness is to be consistent with DM coating thickness in order to provide approximately equal stress from both sides of the DM-AR optical element, there is the second condition of the AR coating feasibility. Typically, optimal AR designs contain layers with thicknesses less than 10 nm. In the present case the AR designs consisting of significantly large number of layers and containing many thin layers have been

Optical Systems Design 2015: Advances in Optical Thin Films V, edited by Michel Lequime,
H. Angus Macleod, Detlev Ristau, Proc. of SPIE Vol. 9627, 96270X · © 2015 SPIE
CCC code: 0277-786X/15/$18 · doi: 10.1117/12.2191120

expected. These layers can cause a problem in the course of the deposition even in the case of high precision deposition systems.

In this work the whole chain including design, production and careful post-production characterization of a complicated double-sided optical element is demonstrated. It is shown how to reach a balance between theoretical expectations and feasibility demands. In Section 2 the theoretical designing of DM and AR coatings is considered. In Section 3 experimental samples and measurement data are presented. In Section 4 post-production characterization of the experimental samples is performed. The final conclusions are presented in Section 5.

2. THEORETICAL DESIGNING

In optical coatings for our DM-AR optical element, Nb_2O_5 is used as high index material and SiO_2 is used as low index material. The substrate is Fused Silica of 15 mm thickness and 75 mm in diameter. Wavelength dependencies of refractive indices of thin-film materials and substrates are described by Cauchy formula:

$$n(\lambda) = A_0 + A_1(\lambda_0/\lambda)^2 + A_2(\lambda_0/\lambda)^4, \quad (1)$$

where $\lambda = 1000$, λ is specified in nanometers. The values of these parameters are presented in Table 1; A_0, A_1, A_2 are dimensionless parameters.

Table 1. Cauchy parameters of thin-film materials and substrates

Material	A_0	A_1	A_2
Nb_2O_5	2.218485	0.021827	3.99968×10^{-3}
SiO_2	1.465294	0	4.71×10^{-4}
Fused Silica	1.449	0.003	3.89×10^{-5}
Glass B260	1.510027	$5.2539\cdot10^{-3}$	$6.328\cdot10^{-5}$

In the DM-AR optical element, the mirror is to be designed first because meeting target specifications on reflectance and GD/GDD is definitely more challenging than AR designing. Synthesis of DM was performed with the help of needle optimization technique incorporated into OptiLayer software[7,8]. As the result a 68-layer DM was obtained. Theoretical reflectance and GD in the spectral range of interest are shown in Fig. 1. Physical thickness of the obtained design is $\mathrm{PhT}_{DM} = 7750$ nm and its optical thickness at the wavelength of 800 nm is $\mathrm{TOT}_{DM} = 13647$ nm. Total physical thicknesses of Nb_2O_5 and SiO_2 layers are $\mathrm{PhT}_{Nb_2O_5} = 2866$ nm and $\mathrm{PhT}_{SiO_2} = 4883$ nm, respectively.

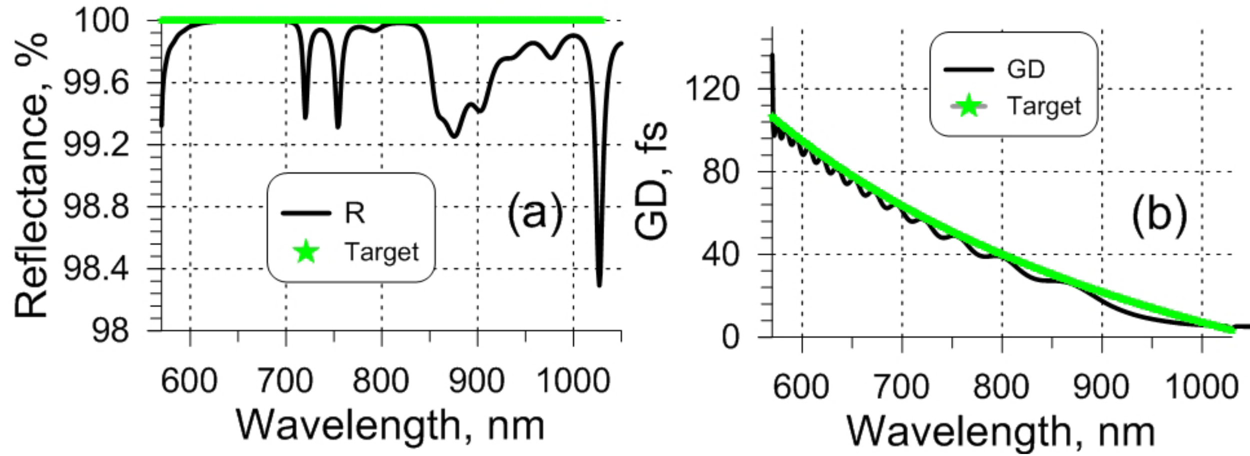

Fig. 1. Theoretical spectral characteristics of the designed DM-AR sample: reflectance (a) and GD (b).

The values PhT_{DM} and TOT_{DM} give estimations for physical and optical thicknesses of AR coating compensating DM stresses. According to [9,10], optimal AR designs consist of quasi-periodic groups of layers (clusters). Optical thickness of one cluster T_c is estimated as:

$$T_c = \frac{\lambda_u}{2}\left[1+\frac{2}{\pi}\arcsin\left(\frac{n_H / n_L - 1}{n_H / n_L + 1}\right)\right] = \frac{1030\text{nm}}{2}\left[1+\frac{2}{\pi}\arcsin\left(\frac{2.25/1.46-1}{2.25/1.46+1}\right)\right] \approx 585\text{nm}, \tag{2}$$

where λ_l, λ_u denote lower and upper boundaries of AR spectral range; n_H, n_L denote refractive indices of high and low index materials taken at the wavelength of 800 nm. The required number of clusters M in the AR design is approximately equal to $\mathrm{TOT}_{DM} / T_c \approx 22-23$.

According to the estimation of the number of layers in the optimal AR designs [11], the number of layers in one cluster is expected to be:

$$N_{cl} = 2\left(\left[\frac{2\cdot T_c}{\lambda_l}\right]+1\right) = 2\left(\left[\frac{1170}{560}\right]+1\right) \approx 6 \tag{3}$$

It means that the total expected number of layers N is about $N \approx N_{cl}\cdot M = 6\cdot 22 = 132$.

The residual reflectance of AR coatings is defined as

$$R_{av} = \frac{1}{\lambda_u - \lambda_l}\int_{\lambda_l}^{\lambda_u} R(\lambda)\, d\lambda. \tag{4}$$

According to the estimation obtained in[12] the minimum residual reflectance achievable foe specified $\lambda_l, \lambda_u, n_H, n_L, n_s$ is 0.07%.

It was found that a 106-layers optimal AR design solution has the parameters close to the estimated ones: $\mathrm{TOT} = 13924$, $\mathrm{PhT} = 7748$ nm. The residual reflectance provided by this 106-layers AR design is 0.073% and it is in the excellent agreement with the theoretically predicted minimum achievable reflectance.

The 106-layer AR design contains seven layers with physical thicknesses less than 10 nm. These layers should be removed in order to avoid problems with deposition of thin layers corresponding to the feasibility requirement. This removal can be done with the help of the procedure known as a *thin layer removal procedure*. In the course of this procedure, the thinnest layer in the design is selected. Then it is substituted with the layer of alternate material having the

same optical thickness. After this substitution the number of layers in the design is decreased by two, since adjacent layers are formed of the same material. This operation increases the merit function that is partially compensated by the following reoptimization procedure, which changes the design only insignificantly. These iterations are repeated until there are no layers thinner than 10 nm in the AR design. As the result of the thin layer removal procedure, a 71-layer AR design has been obtained. The residual reflectance of 71-layer AR design is 0.08 that is also very close to the minimum achievable reflectance value. It is also important to note, that the total physical thicknesses of layer materials are: $PhT_{Nb_2O_5} = 3077$ nm and $PhT_{SiO_2} = 4340$ nm, which is quite close to respective values of the DM mentioned above. Therefore the goal of the DM stress compensation should be also achieved.

3. EXPERIMENTAL SAMPLES AND MEASUREMENTS

The designed DM and AR coatings have been produced using Leybold Optics magnetron sputtering Helios plant, layer thicknesses were controlled using well-calibrated time monitoring [3]. The plant is equipped with two proprietary TwinMags magnetrons and a plasma source for plasma/ion-assisted reactive middle frequency dual magnetron sputtering.

Helios plant is also equipped with broadband monitoring (BBM) system [13]. This system was used in a passive mode for data acquisition only. We performed two deposition runs using Fused Silica substrate for the DM-AR optic production and cheaper B260 Glass substrate as a test witness sample. In the first run, the front sides of Fused Silica and B260 Glass substrates were covered with DM coatings. In the second run, the back side of Fused Silica substrate and front side of another B260 Glass substrate were covered with AR coating. As a result, three samples were obtained: DM coating on B260 Glass substrate (sample DM-B260), AR coating on B260 substrate (sample AR-B260) and DM-AR coatings on Fused Silica substrate (DM-AR- Fused Silica). The BBM data were recorded for DM-B260 and AR-B260 samples.

Turntable of Helios plant has 16 sample positions located at the same distance from the center of rotation. We placed all samples exactly in the middle of two sample positions of turntable. The B260 Glass substrates were placed on the position where BBM system performed measurements.

After the deposition, transmittance data of the produced DM-AR- Fused Silica sample was measured by Perkin Elmer Lambda 950 spectrophotometer in the range from 400 nm to 1200 nm. Theoretical and measured transmittance data related to DM-AR- Fused Silica sample are in a good correspondence. GD of the DM-AR- Fused Silica sample were extracted from the measurements provided by a white light interferometer and processed with specially developed algorithm [14]. The theoretical and measured GD values are consistent.

The surface flatness of the produced samples was measured with homemade Fizeau interferometer. The measurements were performed at He-Ne laser wavelength of 632.8 nm. In the case of DM samples without compensating AR coating the flatness of the surface degraded from $\lambda/10$ to $\lambda/4$. The deposition of the AR coating at the backside of the sample improved surface flatness from $\lambda/4$ to the original value $\lambda/10$, corresponding to the uncoated substrate. Therefore full stress compensation with AR coating is confirmed.

4. POST-PRODUCTION CHARACTERIZATION

According to our previous results [15–17], post-production characterization of the samples was performed on the basis of transmittance scans recorded after deposition of each layer. All transmittance scans were processed simultaneously and triangular algorithm for layer parameters determination [15] was applied. Refractive indices of Nb_2O_5 and SiO_2 thin film materials deposited in Helios plant are stable and known with high accuracy[18,3,4]. This means that refractive index variations are negligible, and deviations between theoretical and experimental data related to deposited samples can be attributed to errors in layer thicknesses only. The post-production characterization algorithm estimating errors in layer thicknesses should be carefully chosen because due to rather large numbers of layers the instability of solutions may readily take place. In order to prevent unreliable characterization solutions, *a priori* information related to errors in layers thicknesses must be taken into account and an appropriate model of possible errors should be chosen. In our case this *a priori* information is that the error level does not exceed 1−2%. Our characterization approach [17] is based on

regularization theory of solving ill-posed problems. It can be formulated as a problem of the Tikhonov's functional minimization that consists of *in situ* discrepancy function with additional stabilizing term:

$$TDF^2 = \frac{1}{mL}\sum_{i=1}^{m}\sum_{j=1}^{L}\left[T\left(X_i,\lambda_j\right)-\hat{T}^{(i)}\left(\lambda_j\right)\right]^2 + \frac{\alpha}{m}\sum_{i=1}^{m}\delta_i^2 . \quad (5)$$

Here $T\left(X_i,\lambda_j\right)$ is the model transmittance for the first i deposited layers assuming that there could be relative random errors $\delta_1,...,\delta_m$ and relative systematic errors $\Delta_{\{H \text{ or } L\}}$ in layer thicknesses:

$$T\left(X_i,\lambda_j\right) = T\left(d_1\left(1+\delta_1+\Delta_H\right),...,d_i\left(1+\delta_i+\Delta_{\{H \text{ or } L\}}\right);n_H\left(\lambda\right),n_L\left(\lambda\right);\lambda\right). \quad (6)$$

In Eq. (5) α is a so-called regularization parameter that is selected to provide a compromise between data fitting and stability of the solution. The second term in Eq. (5) accounts for the stability of solution using *a priori* information that relative random errors cannot be too big. This algorithm is known as the algorithm with quasi-random errors. The regularization parameter was equal to $\alpha = 1$. The relative errors determined by quasi-random errors algorithm in DM-B260 and AR-B260 samples are presented in Fig. 2. Denote X_{DM} and X_{AR} the vectors of layer thicknesses estimated in the course of the post-production characterization process.

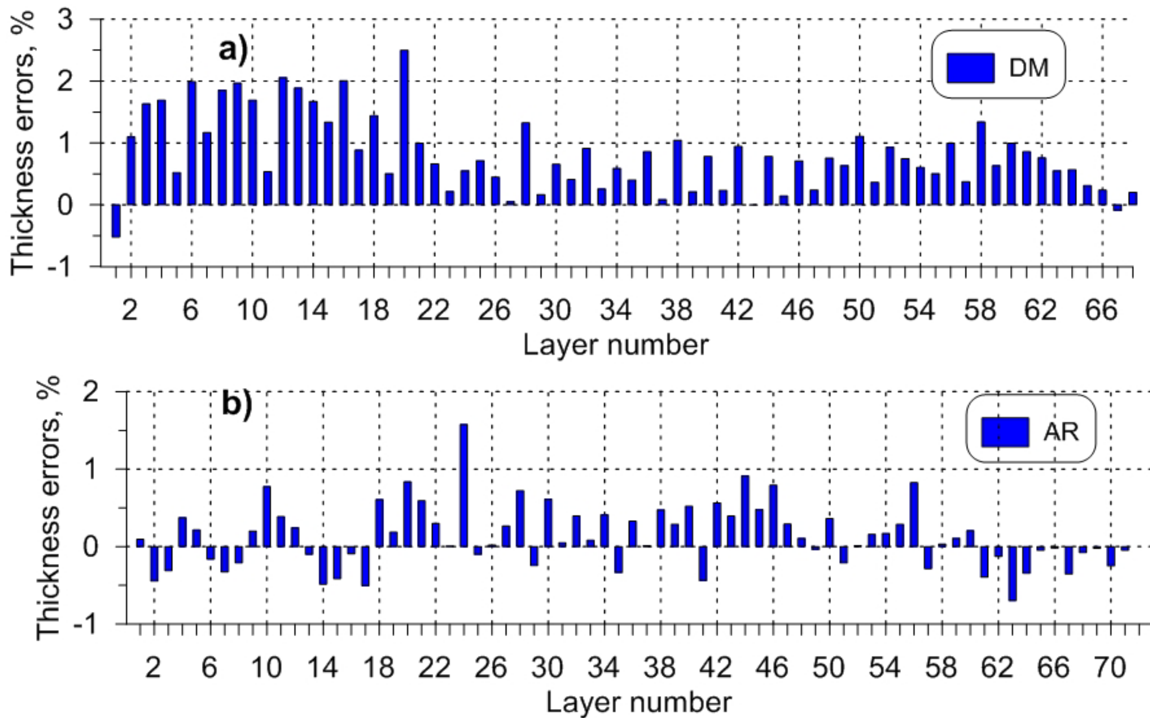

Fig. 2. Relative errors in layer thicknesses in DM-B260 (a) and AR-B260 (b) samples estimated in the course of the post-production procedure.

It has been shown in Ref[17] that the thickness nonuniformity of layers in the samples placed at the witness chip position and at the calotte does not exceed 0.2%. Due to the high uniformity, it can be assumed that the errors in layer thicknesses found on the basis of B260 samples characterization are very close to errors in layer thicknesses in BK7 sample. Substituting the layer thicknesses X_{DM} and X_{AR}, the model transmittance and model GD of the DM-AR-BK7 sample

can be calculated. In Fig. 3 and Fig. 4, good correspondences of model and experimental data related to BK7 sample are presented. This correspondence confirms reliability of our post-production characterization.

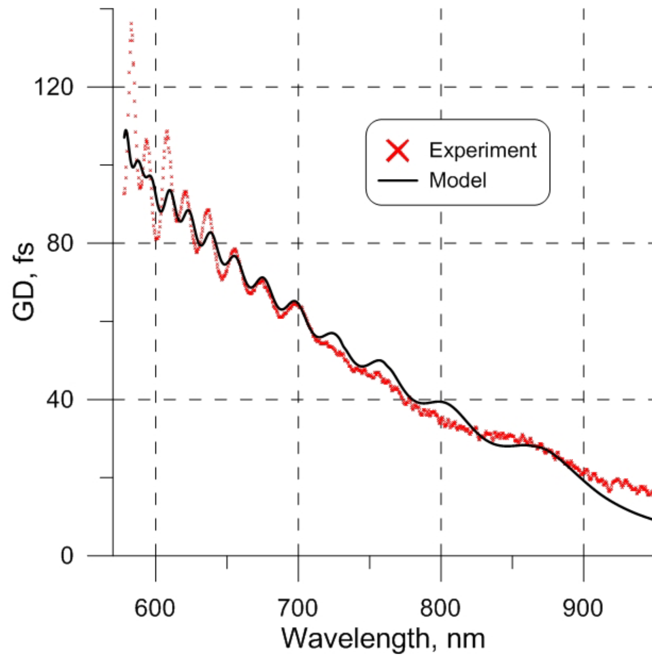

Fig. 3. Correspondence between experimental GD and model GD data.

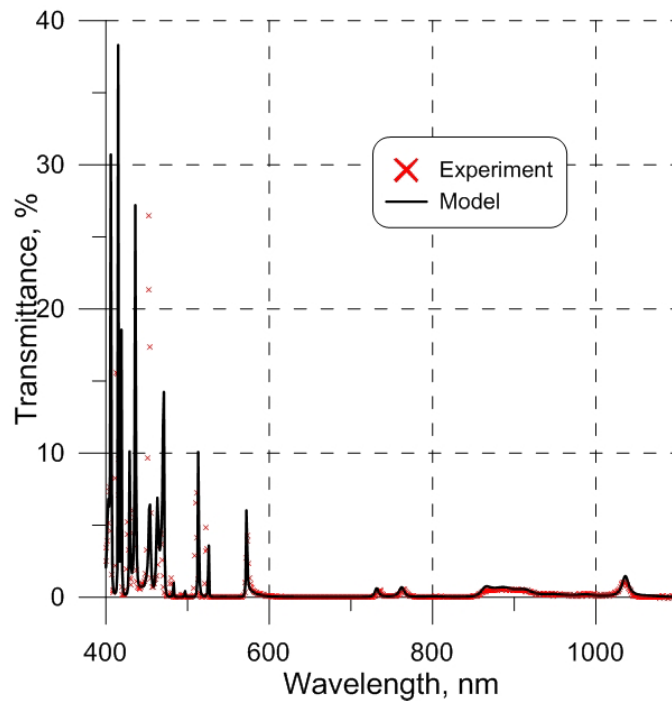

Fig. 4. Correspondence between measured and model transmittance data.

5. CONCLUSIONS

In the present work we demonstrated a unique optical element for laser applications consisting of DM and back-side 71-layer AR coating for reducing the total stress and back reflections. The goals of stress compensation and suppression of back reflections were successfully achieved. Deposition of such double-sided optical elements containing complicated many-layer coatings on both sides of the sample is a challenge for optical coating engineers and designers. The deposition of many-layers dispersive mirrors and anti-reflection coatings requires a deep understanding of the physical processes in the deposition plant and influence of various factors on thickness control, experience in extracting information from *in situ* measurements and making (if necessary) on-line corrections to the deposition process.

ACKNOWLEDGEMENTS

This work is supported by the German Research Foundation Cluster of Excellence, Munich-Centre for Advanced Photonics (http://www.munich-photonics.de). Authors are very grateful to Prof. F. Krausz for fruitful discussions.

REFERENCES

[1] Krausz, F., “Attosecond physics,” Rev. Mod. Phys. **81**(1), 163–234 (2009).

[2] Pervak, V., Teisset, C., Sugita, A., Naumov, S., Krausz, F.., Apolonski, A., “High-dispersive mirrors for femtosecond lasers,” Opt. Express **16**(14), 10220–10233 (2008).

[3] Pervak, V., Tikhonravov, A. V., Trubetskov, M. K., Naumov, S., Krausz, F.., Apolonski, A., “1.5-octave chirped mirror for pulse compression down to sub-3 fs,” Appl. Phys. B **87**, 5–12 (2007).

[4] Pervak, V., “Recent development and new ideas in the field of dispersive multilayer optics,” Appl. Opt. **50**(9), C55 (2010).

[5] Steinmeyer, G., “Femtosecond dispersion compensation with multilayer coatings: toward the optical octave,” Appl. Opt. **45**(7), 1484 (2006).

[6] Hendrix, K., Kruschwitz, J. D. T.., Keck, J., “Optical Interference Coatings Design Contest 2013: angle-independent color mirror and shortwave infrared/midwave infrared dichroic beam splitter,” Appl. Opt. **53**(4), A360 (2014).

[7] Tikhonravov, A. V.., Trubetskov, M. K., “OptiLayer software,” <http://www.optilayer.com>.

[8] Tikhonravov, A. V., Trubetskov, M. K.., DeBell, G. W., “Optical coating design approaches based on the needle optimization technique,” Appl. Opt. **46**(5), 704–710 (2007).

[9] Dobrowolski, J. A., Tikhonravov, A. V., Trubetskov, M. K., Sullivan, B. T.., Verly, P. G., “Optimal single-band normal-incidence antireflection coatings,” Appl. Opt. **35**(4), 644 (1996).

[10] Tikhonravov, A. V., Trubetskov, M. K., Amotchkina, T. V.., Dobrowolski, J. A., “Estimation of the average residual reflectance of broadband antireflection coatings,” Appl. Opt. **47**(13), C124 (2007).

[11] Amotchkina, T., Tikhonravov, A.., Trubetskov, M., “Estimation for the number of layers of broad band anti-reflection coatings,” 19 September 2008, 710104–710104 – 11.

[12] Amotchkina, T. V., “Empirical expression for the minimum residual reflectance of normal- and oblique-incidence antireflection coatings,” Appl. Opt. **47**(17), 3109 (2008).

[13] Ristau, D., Ehlers, H., Gross, T.., Lappschies, M., “Optical broadband monitoring of conventional and ion processes,” Appl. Opt. **45**(7), 1495 (2006).

[14] Amotchkina, T. V., Tikhonravov, A. V., Trubetskov, M. K., Grupe, D., Apolonski, A.., Pervak, V., “Measurement of group delay of dispersive mirrors with white-light interferometer,” Appl. Opt. **48**(5), 949–956 (2009).

[15] Amotchkina, T. V., Trubetskov, M. K., Pervak, V., Schlichting, S., Ehlers, H., Ristau, D.., Tikhonravov, A. V., “Comparison of algorithms used for optical characterization of multilayer optical coatings,” Appl. Opt. **50**(20), 3389–3395 (2011).

[16] Janicki, V., Sancho-Parramon, J., Stenzel, O., Lappschies, M., Görtz, B., Rickers, C., Polenzky, C.., Richter, U., “Optical characterization of hybrid antireflective coatings using spectrophotometric and ellipsometric measurements,” Appl. Opt. **46**(24), 6084 (2007).

[17] Trubetskov, M., Amotchkina, T., Tikhonravov, A.., Pervak, V., “Reverse engineering of multilayer coatings for ultrafast laser applications,” Appl. Opt. **53**(4), A114–A120 (2013).

[18] Pervak, V., Trubetskov, M. K.., Tikhonravov, A. V., “Robust synthesis of dispersive mirrors,” Opt. Express **19**(3), 2371–2380 (2011).